Identification of c-Cbl as a New Ligase for Insulin-like Growth Factor-I Receptor with Distinct Roles from Mdm2 in Receptor Ubiquitination and Endocytosis

Bita Sehat, Sandra Andersson, Leonard Girnita, and Olle Larsson

Department of Oncology and Pathology, Karolinska Institutet, Cancer Center Karolinska, Karolinska University Hospital, Stockholm, Sweden

Abstract

The insulin-like growth factor receptor (IGF-IR) plays several pivotal roles in cancer. Although most studies on the function of the IGF-IR have been attributed to kinase-dependent signaling, recent findings by our group and others have implicated biological roles mediated by ubiquitination of the receptor. As previously reported, the E3 ligases Mdm2 and Nedd4 mediate IGF-IR ubiquitination. Here we show that c-Cbl is a novel E3 ligase for IGF-IR. On ligand stimulation, both Mdm2 and c-Cbl associate with IGF-IR and mediate receptor polyubiquitination. Whereas Mdm2 catalyzed lysine 63 (K63) chain ubiquitination, c-Cbl modified IGF-IR through K48 chains. Mdm2-mediated ubiquitination occurred when cells were stimulated with a low concentration (5 ng/mL) of IGF-I, whereas c-Cbl required high concentrations (50–100 ng/mL). Mdm2-ubiquitinated IGF-IR was internalized through the clathrin endocytic pathway whereas c-Cbl–ubiquitinated receptors were endocytosed via the caveolin route. Taken together, our results show that c-Cbl constitutes a new ligase responsible for the ubiquitination of IGF-IR and that it complements the action of Mdm2 on ubiquitin lysine residue specificity, responsiveness to IGF-I, and type of endocytic pathway used. The actions and interactions of Mdm2 and c-Cbl in the ubiquitination and endocytosis of IGF-IR may have implications in cancer. In addition, identification and functional characterization of new E3 ligases are important in itself because therapeutic targeting of substrate-specific E3 ligases is likely to represent a critical strategy in future cancer treatment. [Cancer Res 2008;68(14):5669–77]

Introduction

Insulin-like growth factor I receptor (IGF-IR), a member of receptor tyrosine kinases (RTK), is a well-recognized mediator of tumor cell proliferation and survival and is associated with the regulation of cell growth, transformation, and apoptosis via phosphatidylinositol 3-kinase-Akt and RAS-RAF-mitogen-activated protein kinase signaling (1–5). Phosphorylation of the receptor has for a long time been considered to be the most important activating signal; however, recent data have shed light on ubiquitination of IGF-IR and its role in mediating biological functions (4, 6–9).

Requests for reprints: Leonard Girnita, CCK R08:04, Karolinska University Hospital, 17176 Stockholm, Sweden. Phone: 46-8-51775242; Fax: 46-8-321047; E-mail: Leonard.Girnita@ki.se.

doi:10.1158/0008-5472.CAN-07-6364

Ubiquitination occurs in a sequence of three enzymatic steps (10, 11). The initial step is the ATP-dependent formation of a thioester bond between the COOH terminus of ubiquitin and the active cysteine residue of a ubiquitin-activating enzyme (E1). Next, the activated ubiquitin is transferred to one of several different ubiquitin-conjugating enzymes (Ubc or E2) in an ATP-independent manner. The E2 enzymes are catalytically similar to E1 in that a thioester bond is formed with ubiquitin. The third and last step in ubiquitination is a reaction catalyzed by a ubiquitin-protein ligase (E3) in which an isopeptide bond between the COOH-terminal glycine of ubiquitin and the ε-amino group of a lysine (K) residue on the target protein is formed. Multiple ubiquitin moieties are transferred through this cascade to generate a polyubiquitin chain. A ubiquitin molecule has seven lysine residues (K6, K11, K27, K29, K33, K48, and K63) that can serve as a base for chain elongation (12). Furthermore, monoubiquitination (transfer of one single ubiquitin to one single lysine) or multiple monoubiquitination (transfer of several monoubiquitin molecules to multiple lysine residues) can occur. Based on current understanding, the K48 polyubiquitin chain, called canonical ubiquitination, makes the substrate recognizable for the 26S proteasome, leading to its degradation (13). Ubiquitin chains based on other lysines, called noncanonical ubiquitination, have diverse functions. The best known example of noncanonical ubiquitination is K63-mediated polyubiquitination, which affects cellular signaling, DNA repair (14, 15), and protein localization (16). c-Cbl is a RING finger domain ligase that directs the multi-monoubiquitination, rather than the polyubiquitination, of activated epidermal growth factor receptor (EGFR) and platelet-derived growth factor (PDGF) receptor and ensures proper endosomal sorting and degradation of receptors in the lysosome (17).

We have previously identified the role of E3 ligase Mdm2 in IGF-IR ubiquitination (6). In this report, we could observe polyubiquitination of IGF-IR in cells overexpressing Mdm2. To our surprise, we could also detect polyubiquitination of the receptor in the absence of Mdm2, indicating the involvement of a separate ligase able to modify the IGF-IR with polyubiquitin chains. We found that c-Cbl induced polyubiquitination of IGF-IR but exhibited several distinct characteristics compared with Mdm2-associated ubiquitination.

Materials and Methods

Reagents. Polyclonal antibodies to IGF-IRβ and EGFR, as well as monoclonal antibodies to EGFR and phospho-caveolin (pY14) and early endosome antigen 1 (EEA-1), used for coimmunoprecipitation and Western blot, were purchased from Cell Signaling Technology. Polyclonal glyceraldehyde-3-phosphate dehydrogenase (GAPDH), monoclonal Mdm2 (D-12), polyclonal p53, monoclonal p53 (D0), and ubiquitin (P4D1) antibodies were purchased from Santa Cruz Biotechnology, Inc. Antibodies to c-Cbl and His-tag, as well as antibodies to phospho-caveolin (pY14) and

EEA-1, used for confocal microscopy, were purchased from BD Transduction Laboratories. Monoclonal antibody to HA epitope was from Roche Diagnostics GmbH. FK1 mouse monoclonal antibody was from Affinity Research Products. Secondary IgM antibody was purchased from Abcam. Secondary antibody for confocal microscopy, Cy3-conjugated donkey anti-rabbit, was purchased from The Jackson Laboratory; Alexa Fluor 488–conjugated goat anti-mouse was from Molecular Probes. Dynabeads protein G were purchased from Invitrogen. Protein G-Sepharose and IgG secondary antibodies were from Amersham. Unless stated otherwise, all other reagents were from Sigma.

Cell cultures. HEK293 cells and human osteosarcoma cell lines U2OS and SAOS2 were cultured in DMEM containing 10% fetal bovine serum (FBS; Life Technologies, Inc.), 10 mmol/L L-Glu, and antibiotics (100 units/mL penicillin and 100 μg/mL streptomycin). U2OS cells and SAOS2 cells were maintained in Iscove's modified Dulbecco's medium supplemented with 10% FBS, 25 mmol/L HEPES, 10 mmol/L L-Glu, and antibiotics (100 units/mL penicillin and 100 μg/mL streptomycin).

Plasmids and small interfering RNA. The HA-c-Cbl plasmid was kindly provided by Dr. W. Langdon (School of Surgery and Pathology, University of Western Australia, Crawley, Australia). The HA-Mdm2 plasmid was a generous gift from Dr. A. Ciechanover (Vascular and Tumor Biology Research Center, The Rappaport Faculty of Medicine and Research Institute, Technion-Israel Institute of Technology, Bat Galim, Haifa, Israel). The DN c-Cbl plasmid, lacking the 17 amino acids including part of the Ring finger domain (18), was a kind gift from Dr. J. Yarden (Department of Biological Regulation, The Weizmann Institute of Science, Rehovot, Israel). The DN Mdm2 plasmid, lacking the ring finger domain (4), was a kind gift from Dr. R.J. Lefkowitz (Department of Medicine, Duke University Medical Center, Durham, NC). Chemically synthesized double-strand small interfering RNAs (siRNA) against c-Cbl (967–985, target sequence 5-CCTCTCT-TCCAAGCACTGA-3) were purchased from Qiagen.

For siRNA knockdown of endogenous Mdm2, siRNA molecules were generated with the Silencer siRNA construction kit (Ambion) and oligonucleotides 5′-AATGATCTTCTAGGAGATTTGCCTGTCTC-3′ (sense) and 5′-AACAAATCTCCTAGAAGATCACCTGTCTC-3′ (antisense).

Transient transfection. The DNA transfection was carried out with Mirus TransIT-LT1 transfection reagent (Mirus Bio Corporation) according to the manufacturer's instructions. Cells were grown to 70% confluency and transfected with 2-μg DNA. The cells were incubated for 24 h in normal growth medium, followed by 24-h incubation in serum-free medium, and then stimulated with 5, 50, or 100 ng/mL of IGF-I. Cells were either lysed in lysis buffer (nondenaturing or denaturing lysis buffer) for immunoprecipitation or Western blot analyses or fixed for confocal analysis. RNA interference experiments were done with TransIT-TKO transfection reagent (Mirus Bio) according to the manufacturer's instructions (Mirus). DNA/RNA cotransfections were carried out with TransIT-LT1 transfection reagent (Mirus) in combination with TransIT-TKO transfection reagent (Mirus) according to the manufacturer's instructions.

Lysis buffers. Nondenaturing lysis buffer [0.5% Triton X-100, 0.5% deoxycholic acid, 150 mmol/L NaCl, 20 mmol/L Tris (pH 7.5), 10 mmol/L EDTA, 30 mmol/L sodium pyrophosphate, 10% glycerol, 50 mmol/L *N*-ethylmaleimide, 1 mmol/L phenylmethylsulfonyl fluoride, protease inhibitor cocktail tablet (Roche), and phosphatase inhibitors 1 and 2 (Sigma)] was used for expression analysis and coimmunoprecipitation analysis. Denaturing lysis buffer TSD [50 mmol/L Tris (pH 7.5), 1% SDS, 5 mmol/L DTT, 50 mmol/L MG132, 50 mmol/L *N*-ethylmaleimide, protease inhibitor cocktail tablet (Roche), and phosphatase inhibitor 1 and 2 (Sigma)] was used for the analysis of ubiquitination. For IGF-IR/phospho-caveolin coimmunoprecipitation, Triton X-100–insoluble, low-density, caveolin-enriched fractions were lysed in *n*-octyl glycoside lysis buffer [10 mmol/L Tris (pH 7.5), 50 mmol/L NaCl, 60 mmol/L *n*-octyl glycoside, 1% Triton X-100, 2 mmol/L EDTA, 0,2% SDS, protease inhibitor cocktail tablet (Roche), and phosphatase inhibitors 1 and 2 (Sigma)].

SDS-PAGE and Western blot analysis. Cell lysates were extracted as described above. Protein samples were dissolved in sample buffer containing 0.0625 mol/L Tris-HCl (pH 6.8), 20% glycerol, 2% SDS, bromophenol blue, and β-mercaptoetanol. Samples corresponding to 50 to 100 μg of cell protein were separated by 4% to 12% gradient SDS-PAGE. After SDS-PAGE, the proteins were transferred onto nitrocellulose membranes (Hybond) and blotted with the indicated antibodies. This was followed by washes and incubation with a horseradish peroxidase (HRP)–conjugated secondary antibody (Amersham) and detected with Hyperfilm-ECL (Amersham).

Immunoprecipitation. For coimmunoprecipitation, cell lysates were extracted as described above with nondenaturing or *n*-octyl glycoside lysis buffer. On addition of 5-μL Dynabeads, the samples were precleared for 1 h at 4°C on a rotator. The protein concentration of the resulting supernatant was determined by the bicinchoninic acid assay (BCA protein assay kit, Pierce) and the same amount of protein was incubated with Dynabeads protein G, previously attached to IGF-IRβ antibody (Cell Signaling), overnight at 4°C. The *n*-octyl glycoside lysis buffer was diluted (1:10) with TNESV buffer [50 mmol/L Tris-HCl (pH 7.5), 1% NP40, 100 mmol/L NaCl, 2 nmol/L EDTA, 10 mmol/L *N*-ethylmaleimide protease inhibitor cocktail tablet (Roche), and phosphatase inhibitor 1 and 2 (Sigma)]. The immunoprecipitates were collected and the supernatant was discarded. The immunoprecipitates were washed thrice with nondenaturing lysis buffer. Sample buffer (1×) for SDS-PAGE was added whereupon the samples were heated for 10 min at 70°C and further analyzed by Western blotting.

For Western blot analysis of IGF-IR ubiquitination, the cells were harvested in 100 μL of denaturing lysis buffer TSD [50 mmol/L Tris-HCl (pH 7.5), 1% SDS, 5 mmol/L DTT, 50 mmol/L *N*-ethylmaleimide, 50 μmol/L MG132, protease inhibitor cocktail tablet (Roche), and phosphatase inhibitors 1 and 2]. The lysates were heated at 98°C for 10 min and spun down in a microcentrifuge at 14,000 rpm. One hundred microliters of supernatant were diluted to a final concentration of 0.1% SDS with TNESV buffer [50 mmol/L Tris-HCl (pH 7.5), 1% NP40, 100 mmol/L NaCl, 2 nmol/L EDTA, 10 mmol/L *N*-ethylmaleimide protease inhibitor cocktail tablet (Roche), and phosphatase inhibitors 1 and 2 (Sigma)]. For Western blot analysis of p53 and EGFR ubiquitination, the cells were treated with the proteasome inhibitor MG132 for 2 h before harvesting.

***In vitro* ubiquitination assay.** *In vitro* ubiquitination of IGF-IR was done as previously described (6) with a few changes. Recombinant glutathione *S*-transferase (GST)-Mdm2 and GST-c-Cbl were expressed in *E. coli* and purified with glutathione-Sepharose (Pierce). IGF-IR was isolated from human melanoma cell line DFB by harvesting in nondenaturing lysis buffer followed by immunoprecipitation of 2 mg of total protein per reaction with anti–IGF-IRβ (Cell Signaling) and protein G-Sepharose (Amersham Pharmacia). Precipitates were extensively washed with LSLD buffer [50 mmol/L NaCl, 0.1% Tween 20, 10% glycerol, 50 mmol/L HEPES, and 20 mmol/L Tris (pH 7.5)], and *in vitro* reactions were done directly on the beads. The *in vitro* reactions contained 20 ng of human recombinant E1 (Boston Biochem), 200 ng of E2 (UbcH5B; Boston Biochem), 2 μg of His-tagged wild-type (wt) or mutated ubiquitin (Boston Biochem), 5 mmol/L ATP, 5 mmol/L $MgCl_2$, 0.1 mmol/L $MnCl_2$, 1 mmol/L DTT, 1 unit of inorganic pyrophosphatase, 10 mmol/L creatine phosphate, and 2.5 units of creatine phosphokinase from rabbit muscle (Sigma), diluted in 50 mmol/L HEPES buffer (pH 7.5) to a final volume of 1 mL. The reactions were incubated on an end-over-end rotator at 37°C for 60 min and were washed thrice with LSLD buffer to eliminate unspecific binding. The immunoprecipitation samples were eluted with 1× NuPAGE LDS Sample Buffer (Invitrogen). Ubiquitinated proteins were detected by Western blot analysis with anti-His-tag polyclonal antibody (BD Transduction Laboratories).

Fluorescence confocal microscopy. Transfected HEK293 cells were plated on 35-mm glass slides in 12-well dishes and serum starved 24 h before stimulation with IGF-I (5 or 100 ng/mL). Cells were fixed in 4% formaldehyde for 20 min, permeabilized with 0.2% Triton X-100 in PBS for 30 min, and blocked with blocking buffer [5% bovine serum albumin (BSA) blocker (Pierce), 5% donkey serum, and 0.3% Triton X-100 in PBS] for 30 min at room temperature. The fixed cells were incubated with primary antibodies, anti–IGF-IRβ (diluted 1:20) and anti EEA-1 (diluted 1:50) or anti–IGF-IRβ (diluted 1:20) and phospho-caveolin-1 (diluted 1:50), overnight. The primary antibody dilution buffer consisted of 1% donkey serum, 0.3% Triton X-100, and 0.1%

NaN_3 in PBS. The appropriate secondary antibodies, donkey anti-rabbit conjugated with Cy3 (1:200 diluted in 2% BSA; The Jackson Laboratory) and Alexa Fluor 488–conjugated goat anti-mouse (1:200 diluted in 2% BSA; Molecular Probes), were used. Slides were mounted using Vectashield with 4′,6-diamidino-2-phenylindole (Vector Labs), and images were acquired and processed as TIFF images in Adobe Photoshop (Adobe Systems, Inc.).

Degradation assay. Protein degradation was assessed by cycloheximide protein chase assay as previously described (7). The stability of IGF-IR was examined by immunoblot analysis at 12 and 24 h after treatment with cycloheximide. The stability of Mdm2 and c-Cbl was analyzed 15 and 60 min after the addition of cycloheximide. The experiment was done in complete culture medium to follow protein down-regulation under physiologic conditions. The protein synthesis of the cells was subsequently inhibited with cycloheximide (50 mg/mL), which was maintained during the entire experiment (7).

Results

c-Cbl is a novel ligase for IGF-IR. To investigate the Mdm2-dependent ubiquitination of IGF-IR in greater detail, two human osteosarcoma cell lines, U2OS and SAOS2, were used. The rationale is that the expression level of Mdm2 differs substantially in these two cell lines: Whereas U2OS expresses high levels of Mdm2, SAOS2 is p53 negative and therefore exhibits very low Mdm2 expression (19, 20). After serum starvation, the cells were stimulated with different doses of IGF-I (0–100 ng/mL) for 10 min followed by denaturing IGF-IR immunoprecipitation and analysis of ubiquitin modification by Western blot with anti-ubiquitin antibodies P4D1 and FK1, as described in Materials and Methods. Whereas P4D1 recognizes both polyubiquitinated and monoubiquitinated proteins, FK1 exclusively recognizes polyubiquitin chains, and not single ubiquitin moieties (17). The emerging theme in studies on RTK ubiquitination is the identification of the specific type of modification (i.e., monoubiquitination, multiubiquitination, and/or polyubiquitination) because this may have relevance for the physiologic outcome. We can observe that IGF-IR is indeed polyubiquitinated as a response to both low-dose and high-dose ligand stimulation (Fig. 1*A*). Interestingly, in U2OS cells expressing high levels of Mdm2, IGF-IR ubiquitination occurred after stimulation with low dose (5 ng/mL) and intermediate dose (50 ng/mL) of IGF-I, but did not appear on stimulation with high dose (100 ng/mL) of the ligand (Fig. 1*A*). In SAOS2 cells, with very low expression of Mdm2, ubiquitination of the receptor was only seen after stimulation with 50 to 100 ng/mL of IGF-I. Furthermore, overexpression of Mdm2 in SAOS2 cells and knockdown of Mdm2 in U2OS completely changed the responsiveness to IGF-I for IGF-IR ubiquitination. Whereas Mdm2 overexpression in SAOS2 induced maximal receptor ubiquitination at low concentration of IGF-I, high ligand concentration was required in U2OS treated with siMdm2 (Fig. 1*B*). These data raise several different possibilities: (*a*) high ligand stimulation is required to recruit sufficient amounts of Mdm2 to the IGF-IR in SAOS2 cells due to very low expression of

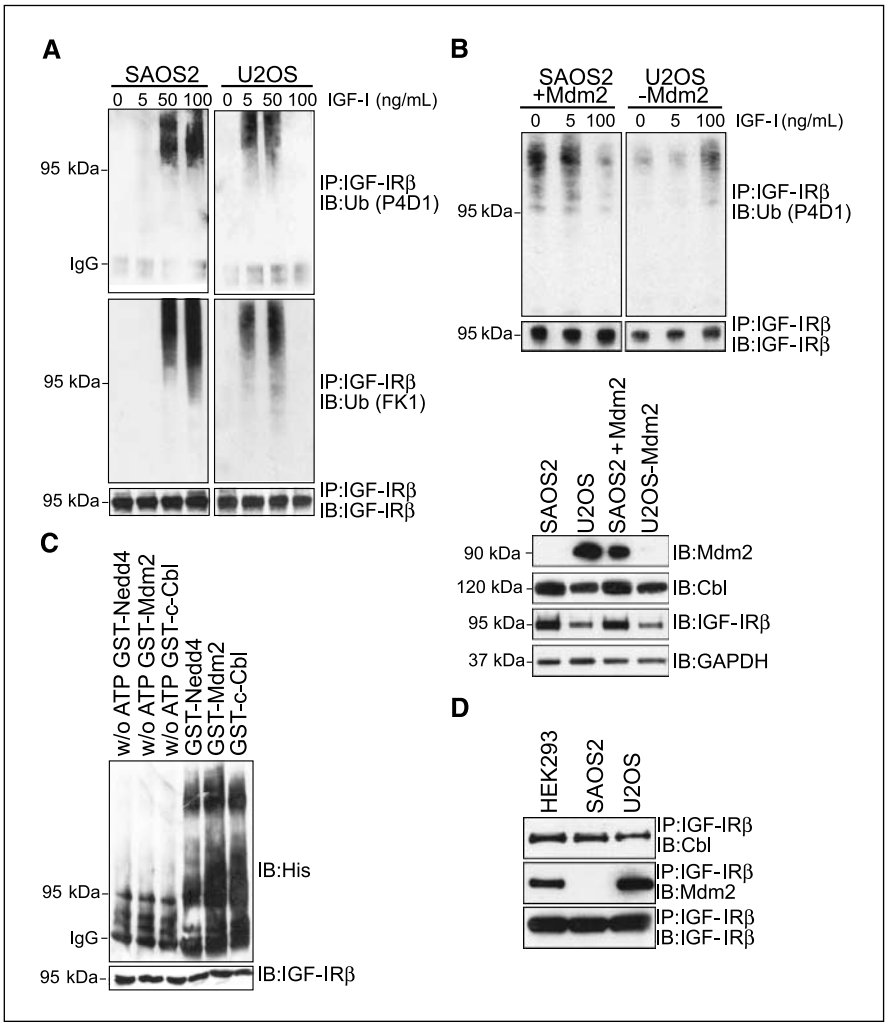

Figure 1. Mdm2 and c-Cbl mediate IGF-IR polyubiquitination. *A,* the two human osteosarcoma cell lines SAOS2 ($TP53^{-/-}$) and U2OS were serum starved for 24 h and stimulated with different doses of IGF-I (0–100 ng/mL) for 10 min. IGF-IR was immunoprecipitated and detected with anti-P4D1 (detecting total ubiquitin) or FK1 (detecting polyubiquitin chains) and anti–IGF-IR. *B, top,* SAOS2 cells were transfected with Mdm2 (+*Mdm2*) for 48 h and U2OS cells were transfected with siMdm2 (−*Mdm2*) for 48 h. Cells were serum starved for 24 h and stimulated for 10 min with IGF-I (0–100 ng/mL). IGF-IR was immunoprecipitated and detected with P4D1 and IGF-IR antibodies. *Bottom,* expression levels of Mdm2, c-Cbl, and IGF-IR in SAOS2 (basal and after Mdm2 overexpression) and U2OS (basal and after Mdm2 knockdown). GAPDH was used as a loading control. *C, in vitro* ubiquitination of IGF-IR was done as described in Materials and Methods. Recombinant GST-Mdm2, GST-Nedd4, and GST-c-Cbl, as well as IGF-IR (isolated from DFB), were incubated together with His-tagged wild-type ubiquitin. Ubiquitinated proteins were detected by Western blot with anti–His-tag polyclonal antibody. *D,* SAOS2, U2OS, and HEK293 cells were grown under basal conditions. IGF-IR was immunoprecipitated and analyzed for c-Cbl, Mdm2, and IGF-IR by Western blot.

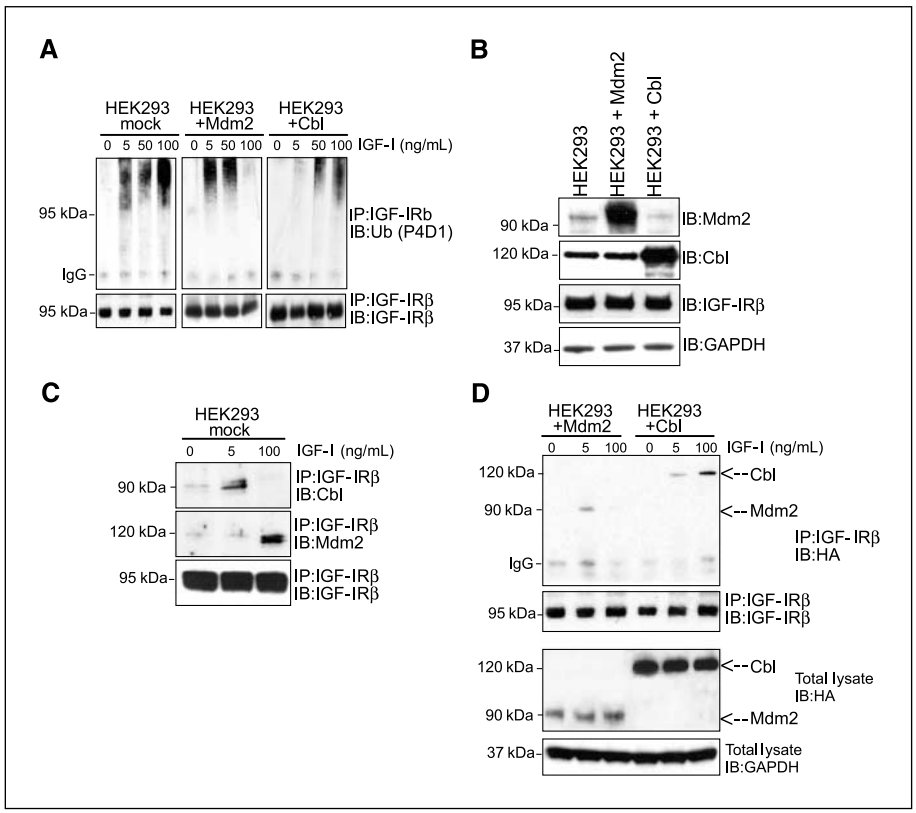

Figure 2. Ligand dose-dependent ubiquitination and association of ligases with IGF-IR. *A,* HEK293 cells were transfected with empty vector (*mock*), Mdm2 (+*Mdm2*), or c-Cbl (+*Cbl*) for 48 h, serum starved for 24 h, and stimulated with different doses of IGF-I (0–100 ng/mL) for 10 min. IGF-IR was immunoprecipitated and detected by P4D1 and IGF-IR antibodies. *B,* the expression of Mdm2, c-Cbl, IGF-IR, and GAPDH was analyzed in mock-transfected, Mdm2-transfected, and c-Cbl–transfected HEK293 cells. The experiments were repeated with similar results. *C,* mock-transfected HEK293 cells were serum starved for 24 h and stimulated with different doses of IGF-I for 10 min. IGF-IR was immunoprecipitated and analyzed with antibodies to c-Cbl, Mdm2, and IGF-IR. *D,* HEK293 cells were transfected with either HA-tagged Mdm2 or HA-tagged c-Cbl for 48 h. The cells were serum starved for 24 h and stimulated with different doses of IGF-I for 10 min. IGF-IR was immunoprecipitated and analyzed with antibodies to HA or IGF-IR. HA and GAPDH from total lysate were used as controls.

Mdm2; (*b*) another/other ligase(s) also induce(s) ubiquitination of IGF-IR and this/these ligase(s) require(s) high ligand stimulation; or (*c*) this is due to other differences in these two cell lines. To investigate this issue in a "cleaner system," we performed *in vitro* (cell-free) ubiquitination assay including three different ligases: Mdm2, Nedd4, and c-Cbl. Whereas Mdm2 and Nedd4 are already known E3 ligases involved in IGF-IR ubiquitination (6, 8), c-Cbl plays a pivotal role in mediating ligand-induced ubiquitination of many other RTKs (21–24). As can be seen from Fig. 1*C*, c-Cbl induced IGF-IR ubiquitination in the *in vitro* system.

We also investigated whether c-Cbl is associated with IGF-IR. This experiment was done under basal conditions (i.e., in the presence of 10% serum). The β subunit of IGF-IR was isolated from U2OS and SAOS2 as well as from HEK293 cells by immunoprecipitation and detected by Western blot. As shown in Fig. 1*D*, c-Cbl is associated with IGF-IR in all three human cell lines. The findings that c-Cbl ubiquitinates and associates with IGF-IR are novel and deserve further detailed analysis.

Mdm2-induced versus c-Cbl–induced IGF-IR ubiquitination. To evaluate if c-Cbl mediates IGF-IR ubiquitination *in vivo* (cell system), HEK293 cells were transiently transfected with human HA-Mdm2 or HA-c-Cbl, serum starved, and stimulated with different doses of IGF-IR (0–100 ng/mL). IGF-IR was immunoprecipitated under denaturing conditions and analyzed for ubiquitin modification. In mock-transfected HEK293 cells, IGF-IR was ubiquitinated in response to both low and high doses of IGF-I (Fig. 2*A*). When Mdm2 was overexpressed, the receptor was ubiquitinated at 5 to 50 ng/mL, whereas c-Cbl overexpression mediated ubiquitination at 50 to 100 ng/mL IGF-I (Fig. 2*A*). This suggests that ubiquitination of IGF-IR at low IGF-I dose is mediated by Mdm2 and at high dose by c-Cbl. The expression levels of Mdm2, c-Cbl, and IGF-IR are shown in Fig. 2*B*.

Consistent with the ubiquitination data, we found that association of Mdm2 with IGF-IR occurs after 5 ng/mL IGF-I stimulation, whereas c-Cbl-IGF-IR association appears mainly after stimulation with high doses of ligand (100 ng/mL; Fig. 2*C*). The association pattern of Mdm2 and c-Cbl with IGF-IR was independent of the overexpression of the two ligases (Fig. 2*D*).

We also performed cotransfection experiments in which either the plasmid DNA of one ligase and siRNA towards the other ligase or the plasmid of one ligase and dominant negative (DN) plasmid of the other ligase were introduced simultaneously. As can be seen in Fig. 3*A*, transfection of c-Cbl-siRNA, alone or along with Mdm2 overexpression, increased IGF-IR ubiquitination at a low dose of IGF-I, whereas siRNA against Mdm2, alone or in combination with c-Cbl overexpression, increased ubiquitination after stimulation with high-dose IGF-I (Fig. 3*A, top*). Similar effects were achieved when the activities of Mdm2 and c-Cbl were down-regulated by DN constructs (Fig. 3*A, bottom*). The expression levels of Mdm2, c-Cbl, and IGF-IR are shown in Fig. 3*B*. To exclude the possibility that the overexpression of one ligase promotes the ubiquitination-mediated degradation of the other ligase, we performed cycloheximide protein chase assay. Whereas the overexpression of both ligases increases the degradation rate of IGF-IR, the overexpression of c-Cbl has no effect on degradation of Mdm2, and vice versa (Fig. 3*C*). Taken together, these results emphasize the roles of Mdm2 and c-Cbl in the ubiquitination of IGF-IR and suggest that they do not form a coregulation loop.

Furthermore, we evaluated whether overexpression of either Mdm2 or c-Cbl modifies the ligase activity of the other by analyzing the ubiquitination of known substrates of both ligases (p53 and EGFR as substrates for Mdm2 and c-Cbl, respectively). On c-Cbl overexpression in U2OS, the ubiquitination of p53 remains unchanged, indicating that Mdm2 activity is not affected (Fig. 3*D,*

top). Moreover, the enzymatic activity of c-Cbl is not modified by Mdm2 overexpression as shown in Fig. 3*D* (*bottom*).

c-Cbl mediates the canonical ubiquitination and Mdm2 noncanonical ubiquitination of IGF-IR. Considering our finding that IGF-IR is polyubiquitinated (Fig. 1*A*), we further examined the ligase activities of Mdm2 and c-Cbl in a series of *in vitro* reactions using mutated ubiquitin. We performed these experiments to specifically determine whether Mdm2 and c-Cbl use different lysine linkages (K48 or K63) in polyubiquitin chain formation. Briefly, human IGF-IR (isolated from melanoma cells, DFB), GST-tagged Mdm2, or GST-tagged c-Cbl was incubated *in vitro* together with recombinant human E1, the E2 enzyme UbcH5B, ATP, as well as His-tagged wt or mutated ubiquitin as indicated. If one lysine mutant (K48R or K63R) blocks ubiquitination, it would suggest that this specific lysine linkage (K48 or K63) is used. Mutated ubiquitin with only one lysine left to be conjugated, here indicated as K48 only or K63 only, was also used as an additional control. The specificity of the assay was confirmed using samples without ATP as negative controls. As seen in Fig. 4, Mdm2 together with wt ubiquitin caused ubiquitination of IGF-IR. It also led to a clear accumulation of K63 polyubiquitination (K63 only). However, when K63R was used, no ubiquitination occurred (Fig. 4). Furthermore, whereas the K48-only mutant did not cause IGF-IR ubiquitination via Mdm2, the K48R did. These results indicate that Mdm2

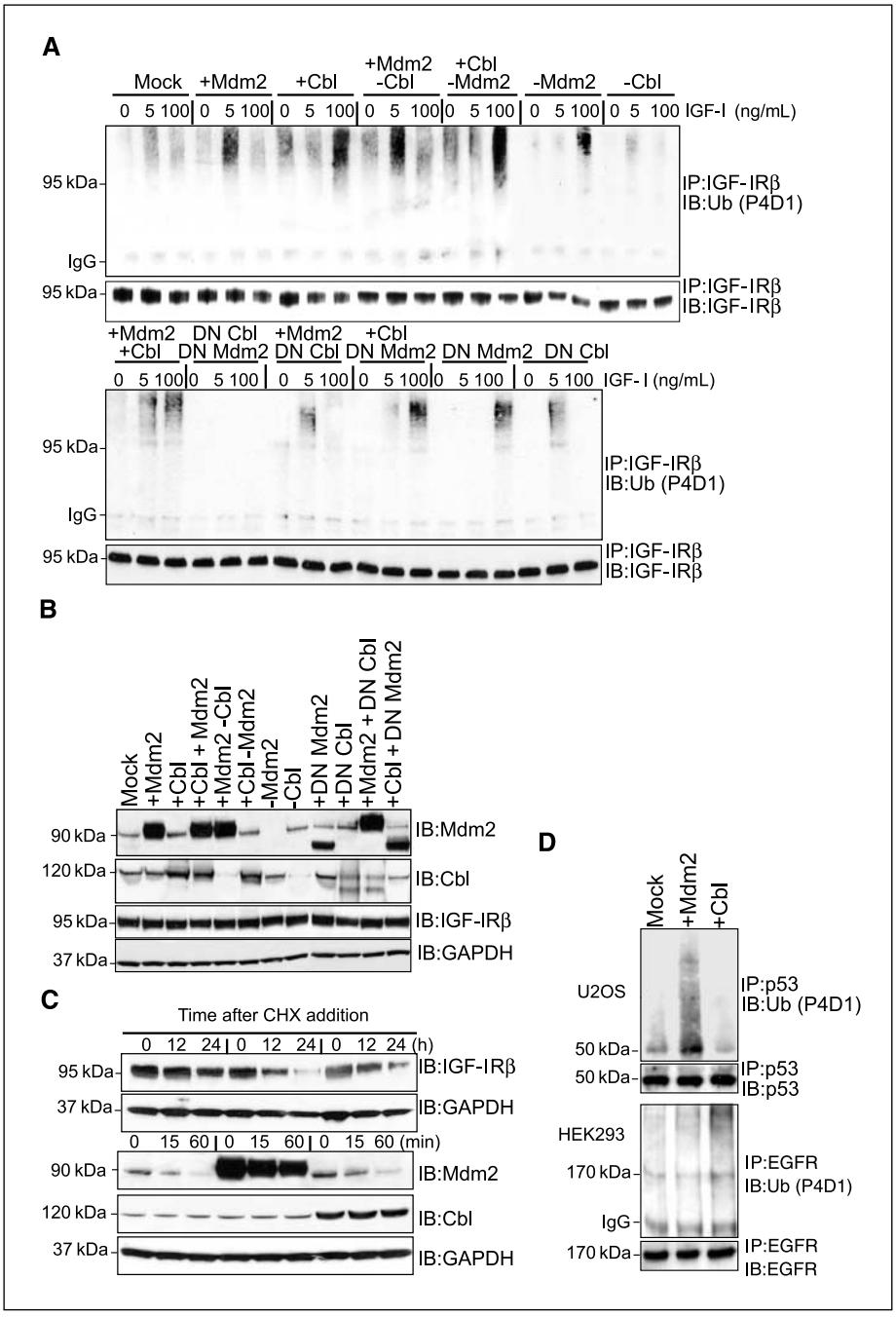

Figure 3. Ligand dose-dependent ubiquitination of IGF-IR. *A,* HEK293 cells were transfected either with wt or DN forms of Mdm2 (*DN Mdm2*) or c-Cbl (*DN Cbl*) for 48 h or with siRNA to Mdm2 (−*Mdm2*) or c-Cbl (−*Cbl*), or the indicated combinations, for 48 h. Cells were serum starved for 24 h and stimulated for 10 min with IGF-I (0–100 ng/mL). IGF-IR was immunoprecipitated and detected with P4D1 ubiquitin and IGF-IRβ antibodies. *B,* expression of Mdm2, c-Cbl, and IGF-IR in samples from the experiments described in *A*. GAPDH was used as a loading control. *C,* IGF-IR, Mdm2, and c-Cbl derived from HEK293 cells were detected by Western blot 48 h after transfection with empty vector (mock), Mdm2, or c-Cbl. Cycloheximide (*CHX*; 50 μg/mL) was added for the indicated times. GAPDH was used as a loading control. *D,* U2OS and HEK293 cells were transfected with empty vector (mock), Mdm2, or c-Cbl for 48 h. EGFR or p53 was immunoprecipitated and detected with P4D1 ubiquitin and p53 or EGFR antibody.

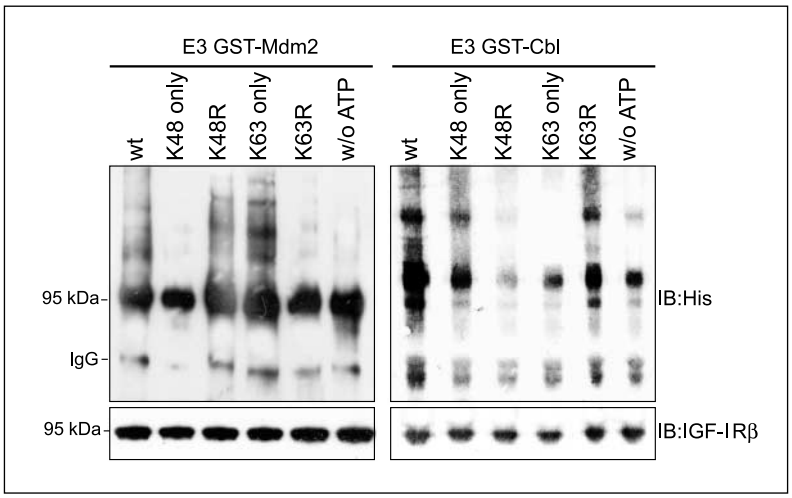

Figure 4. Canonical and noncanonical polyubiquitination. *In vitro* ubiquitination of IGF-IR was done as described in Materials and Methods. Recombinant GST-Mdm2 and GST-Cbl, as well as IGF-IR (isolated from DFB), were incubated together with wild-type ubiquitin or the indicated mutants. Ubiquitinated proteins were detected by Western blot with anti-His polyclonal antibody. The experiments were repeated with similar results.

mediates K63 polyubiquitination. Alternatively, when *in vitro* reactions were conducted using c-Cbl as ligase together with wt or K48 only ubiquitin, typical polyubiquitin smears of the IGF-IR were detected (Fig. 4). Additionally, the mutant ubiquitin K63R, which has all the lysines but K63, could be conjugated to the IGF-IR. In contrast, the ubiquitin mutant K63 only and K48R were not conjugated. Together, these experiments suggest that Mdm2 mediates the formation of K63 polyubiquitin chains, whereas c-Cbl mediates the canonical ubiquitination (K48 polyubiquitin chain) of IGF-IR.

Mdm2 and c-Cbl mediate IGF-IR internalization through different pathways. To discriminate whether ubiquitination of IGF-IR through different ligases may play a role in regulating internalization, we looked at IGF-IR colocalization with the lipid raft/caveolar marker tyrosine phospho-caveolin-1 (pY14) and the early endosome marker early endosome autoantigen 1 (EEA-1) using coimmunoprecipitation and immunofluorescence confocal microscopy. Mock-transfected HEK293 cells and HEK293 cells transfected with Mdm2 and c-Cbl were serum starved for 24 hours and stimulated with 5 or 100 ng/mL of IGF-I. IGF-IR internalization was analyzed by double staining to assess the extent of colocalization of IGF-IR/phospho-caveolin-1 (Fig. 5*A*) and IGF-IR/EEA-1 (Fig. 6*A*), respectively. In starved HEK293 cells, caveolin-1 was not phosphorylated and, therefore, could not be seen. After stimulation with 5 ng/mL IGF-I, caveolin-1 was phosphorylated and, therefore, detectable as green dots in the cell membrane, but no colocalizations could be found. However, after stimulation with 100 ng/mL IGF-I, IGF-IR colocalization with phospho-caveolin-1 (yellow) occurred in perinuclear regions (3rd and 5th columns represent magnified characteristic square-labeled fields from 2nd and 4th columns). This result suggests that IGF-IR is partitioned into caveolae on stimulation with high-dose IGF-I. Interestingly, whereas Mdm2 overexpression decreased IGF-IR/phospho-caveolin-1 colocalization, at both low-dose and high-dose IGF-I, overexpression of c-Cbl increased this colocalization (Fig. 5*A*). On the other hand, in mock-transfected cells, IGF-IR/EEA-1 colocalization was found mainly after low-dose IGF-I stimulation but was remarkably increased after Mdm2 overexpression. The IGF-IR/EEA-1 colocalization was decreased by c-Cbl overexpression (Fig. 6*A*).

The results from confocal imaging shown in Figs. 5*A* and 6*A* are confirmed by coimmunoprecipitation experiments (Figs. 5*B* and 6*B*). HEK293 cells, transfected with empty vector (mock), wt Mdm2, wt c-Cbl, DN Mdm2, and DN c-Cbl, on starvation and stimulation with 0, 5, or 100 ng/mL IGF-I, were immunoprecipitated with either phospho-caveolin (Fig. 5*B*) or IGF-IR (Fig. 6*B*) and detected with IGF-IR and EEA-1 antibodies, respectively. Consistently, IGF-IR was associated with phospho-caveolin after high-dose ligand stimulation, which increased on inhibition of Mdm2 by DN Mdm2 overexpression and c-Cbl overexpression (Fig. 5*B*). Overexpression of Mdm2 and DN c-Cbl abolished this interaction. Furthermore, IGF-IR/EEA-1 association occurred after low-dose IGF-I stimulation, which slightly increased on Mdm2 and DN c-Cbl overexpression. Overexpression of c-Cbl and DN Mdm2 inhibited this interaction.

Taken together, our data indicate that IGF-IR after c-Cbl overexpression associates mainly with phospho-caveolin but poorly with clathrin, whereas on Mdm2 overexpression the opposite response occurs. Consistent with Fig. 6, the IGF-IR interaction with EEA-1 was strongest after stimulation with 5 ng/mL IGF-I, and the IGF-IR interaction with phospho-caveolin most prominent at 100 ng/mL.

Discussion

In the present work, we have expanded our previous observation that Mdm2 functions as an E3 ligase for ubiquitination of IGF-IR (4), and show that c-Cbl, a known E3 ligase for other RTKs such as EGFR, PDGF receptor, and colony-stimulating factor-1 receptor, is also a ligase for IGF-IR. Our present data strongly suggest that the two ligases, Mdm2 and c-Cbl, play distinct roles in the ubiquitination of the receptor. By inhibiting one ligase using siRNA or DN constructs and overexpressing the other, we show that Mdm2-mediated IGF-IR ubiquitination occurs after low-dose IGF-I stimulation, whereas c-Cbl–mediated ubiquitination occurs following high-dose IGF-I stimulation. By overexpressing only Mdm2, we found that IGF-IR ubiquitination was strongly increased at low-dose IGF-I stimulation, whereas ubiquitination at high dose could not be detected. The opposite occurred after c-Cbl overexpression, which suggests that the function of the corresponding endogenous ligase could be restricted in this system. However, by overexpressing both Mdm2 and c-Cbl simultaneously, the IGF-IR seems to be ubiquitinated at both low dose and high dose at similar levels. Hence, it remains to be determined if Mdm2 and c-Cbl cooperate or compete with each other in ubiquitinating the IGF-IR.

Both Mdm2 and c-Cbl associate with IGF-IR when stimulated with low-dose IGF-I; however, on high-dose stimulation, this

interaction is strongly enhanced in c-Cbl–overexpressing cells whereas it disappeared in cells that overexpress Mdm2. Furthermore, both ligases interact with IGF-IR under basal conditions, suggesting that they may play physiologic roles in IGF-IR function.

Our findings indicate that both ligases are capable of polyubiquitinating IGF-IR. The next question raised was if there is a preference for Mdm2- and c-Cbl–mediated polyubiquitination when it comes to the choice of the lysine residue used to form the ubiquitin chain.

Polyubiquitination and monoubiquitination have been reported to be involved in the internalization of several membrane proteins (25). Haglund et al. (17) showed that the EGFR is multiply monoubiquitinated. However, Huang et al. (26) provided direct evidence, using tandem mass spectrometry, that more than 50% of all EGFR-bound ubiquitin was in the form of polyubiquitin chains. These polyubiquitin chains are primarily linked through K63 (26).

Using various mutated ubiquitins in an *in vitro* ubiquitination assay, we show that Mdm2 modifies IGF-IR with K63 chain, whereas c-Cbl causes K48 ubiquitination of the receptor. We did not perform a corresponding *in vivo* experiment (i.e., studying IGF-IR ubiquitination after transfection with wt and mutated ubiquitin) due to the complexity of this system. The limitations of the *in vivo* approach are due to (*a*) high levels of endogenous ubiquitin expression that can interfere with the incorporation of mutant ubiquitin (26); (*b*) the abundance of cellular deubiquitination enzymes, which may render some ubiquitin chains more unstable than others (27–29); and (*c*) mammalian cells expressing mutant ubiquitin, which respond very differently from cells expressing only wild-type ubiquitin (30).

Ubiquitination has been reported to play an important role in both the internalization and sorting of receptors (31). Plasma membrane receptors can be endocytosed through clathrin-dependent or clathrin-independent (caveolae-mediated lipid raft route) pathways. Sigismund et al. (32) showed that EGFR, when stimulated with low-dose EGF, is not ubiquitinated and the receptor is internalized through the clathrin pathway. At higher concentrations of ligand, however, a substantial fraction of the EGFR is endocytosed through the lipid raft–dependent route as the receptor becomes ubiquitinated. It has also been reported that IGF-IR is located in lipid rafts/caveolae of the plasma membrane and can directly interact with and phosphorylate the major protein component in caveolae, caveolin-1, at tyrosine 14 (33). Furthermore, it has been reported that IRS-1, a substrate for insulin receptor and IGF-IR, colocalizes with phospho-caveolin after IGF-I stimulation (34). Therefore, one can speculate that the interaction between phospho-caveolin and IGF-IR may occur via IRS-1. The caveolin-1 association and phosphorylation seems to be IGF-IR specific because caveolin-1 was not recruited to the insulin receptor in IGF-IR knockout cells (35). Moreover, Huo et al. (36) showed that disruption of lipid rafts/caveolae by depleting cellular cholesterol blocks the IGF-I receptor signaling in 3T3-L1 preadipocytes. Thus, there is evidence that IGF-IR can be internalized via both clathrin-dependent and caveolin-dependent routes.

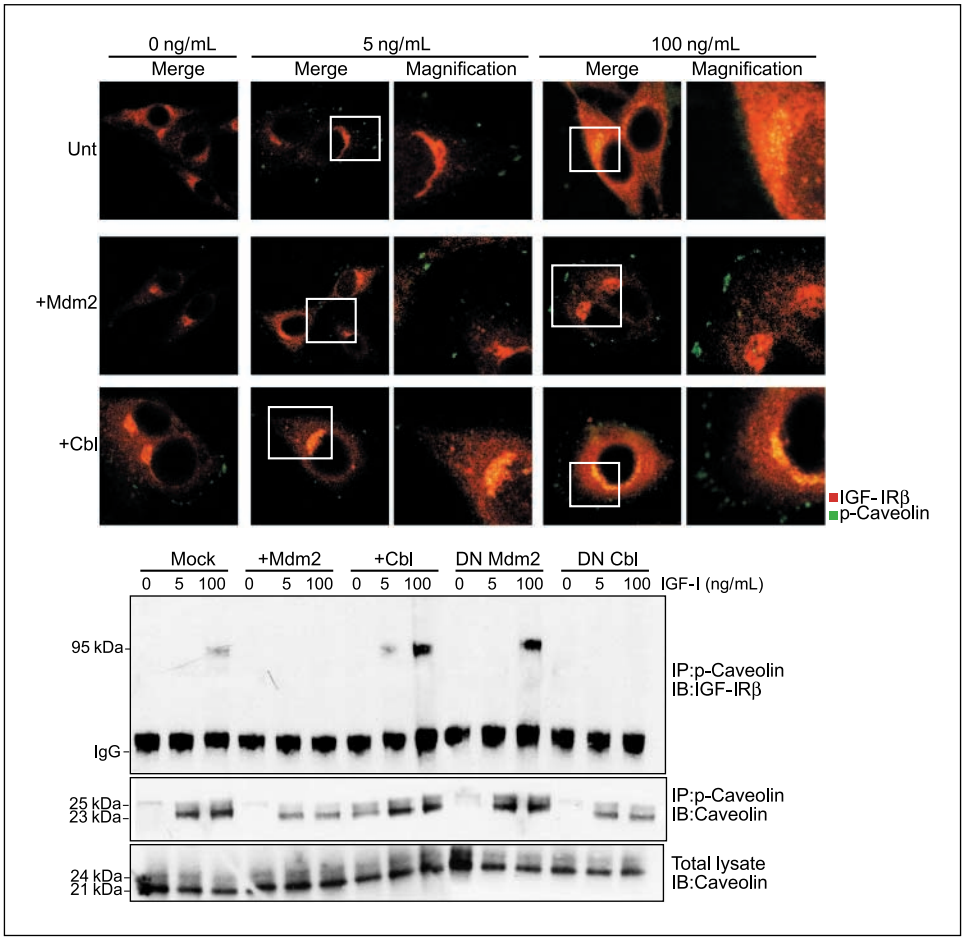

Figure 5. Mediation of the caveolin internalization pathway. *A,* HEK293 cells were transfected with empty vector (mock), Mdm2, or c-Cbl. The cells were serum starved and stimulated with IGF-I (0, 5, or 100 ng/mL) for 10 min. The cells were fixed and stained with both anti–phospho-caveolin-1 and anti–IGF-IR antibodies. Immunofluorescence confocal microscopy was done. *Columns 3* and *5,* magnified fields indicated by squares in *columns 2* and *4*, respectively. *B,* HEK293 cells were transfected either with empty vector (mock) or with wt or DN forms of Mdm2 or c-Cbl. The cells were serum starved and stimulated as in *A*. After immunoprecipitation of phospho-caveolin, the samples were analyzed for IGF-IR and caveolin by Western blot. Caveolin from total lysate was used as a loading control. The experiments were repeated with similar results.

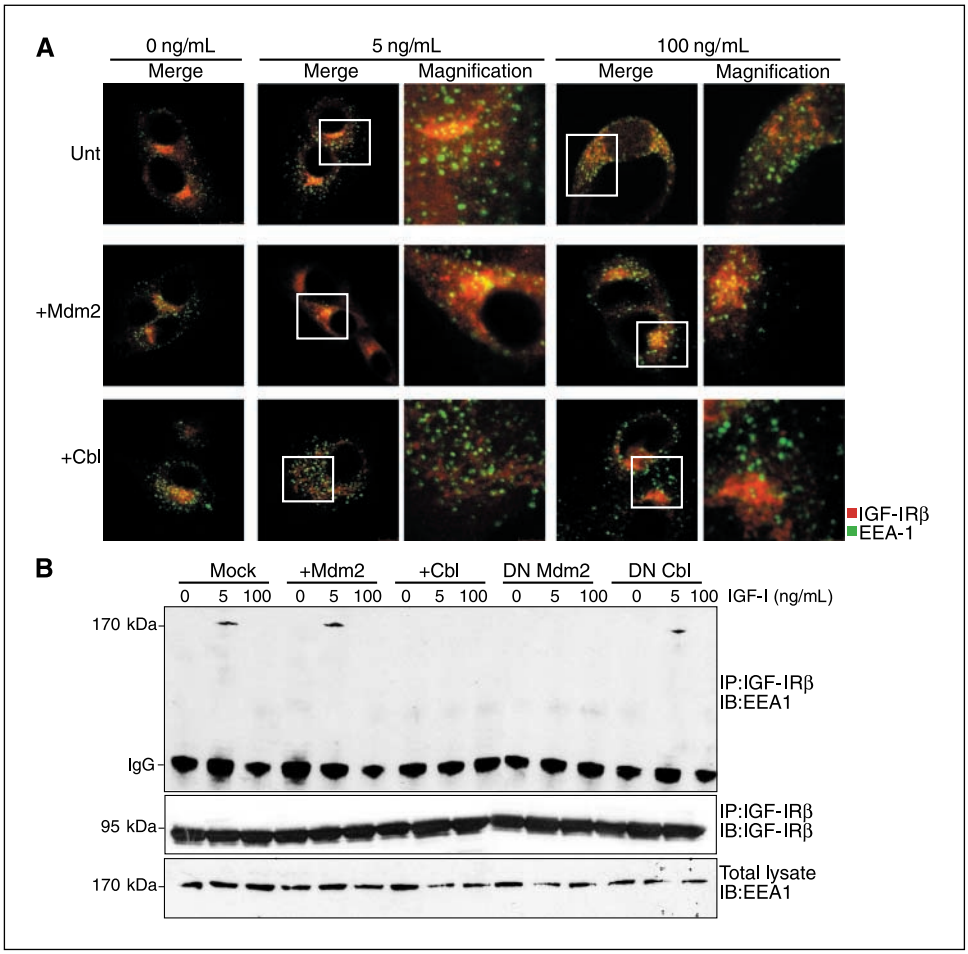

Figure 6. Mediation of the clathrin internalization pathway. *A,* HEK293 cells were transfected with empty vector (mock), Mdm2, or c-Cbl. The cells were serum starved and stimulated with IGF-I (0, 5, or 100 ng/mL) for 10 min. The cells were fixed and stained with anti–EEA-1 and anti–IGF-IR antibodies. Immunofluorescence confocal microscopy was done. *Columns 3* and *5,* magnified fields indicated by squares in *columns 2* and *4*, respectively. *B,* HEK293 cells were treated as described in Fig. 5*B*. After immunoprecipitation of IGF-IR, the samples were analyzed for EEA-1 and IGF-IR by Western blot. EEA-1 was used as a loading control. The experiments were repeated with similar results.

It has also been shown that the adapter protein β-arrestin, responsible for bringing the Mdm2 ligase to the IGF-IR (4, 9), is important for regulating the clathrin-mediated endocytosis of the receptor (37), and that tyrosine-phosphorylated c-Cbl and c-Cbl–associated protein are recruited to lipid rafts (38). Based on these findings, we hypothesized that Mdm2- and c-Cbl–mediated ubiquitination of IGF-IR may induce different internalization pathways.

Interestingly, our results show that IGF-IR has two alternative internalization pathways that are dependent on ligand dosage. The emergence of IGF-IR/phospho-caveolin colocalization correlates with the IGF-IR/Cbl colocalization, and IGF-IR/EEA-1 interaction resembles IGF-IR/Mdm2 interaction. The fact that c-Cbl inhibition abolishes the colocalization of IGF-IR with phospho-caveolin supports the idea that Cbl-mediated IGF-IR ubiquitination is crucial for IGF-IR internalization via the lipid raft pathway. Accordingly, the IGF-IR/phospho-caveolin colocalization increases on c-Cbl overexpression; however, this interaction is abrogated after Mdm2 overexpression, which suggests that endogenous c-Cbl may be negatively regulated by the high levels of Mdm2.

Our results also indicate the involvement of Mdm2/IGF-IR interaction in the clathrin-dependent internalization pathway. Conversely, we also show that endogenous Mdm2 may be negatively inhibited by c-Cbl overexpression.

Taken together, Mdm2-mediated IGF-IR ubiquitination targeted the receptor to endosomes, whereas c-Cbl–mediated IGF-IR ubiquitination was internalized via the caveolin/lipid raft route.

It remains to be determined whether the choice of internalization route depends directly on the association of the ligase with putative adapter proteins important for these internalization pathways or if the endocytic pathway route depends directly on the canonical versus noncanonical ubiquitination of the target. The effect of the two different pathways on the biological functions of IGF-IR warrants further investigation.

In conclusion, the results presented in this study show that both Mdm2 and c-Cbl are E3 ligases associating with and polyubiquitinating the IGF-IR in response to ligand stimulation. However, they differ in their responsiveness to ligand stimulation and ubiquitin lysine residue specificity in linkages of the polyubiquitin chains. From a functional point of view, they mediate different endocytic pathways. The interplay between Mdm2 and c-Cbl in the ubiquitination of IGF-IR may be important in cancer biology and requires further investigation. In addition, the identification and functional characterization of new E3 ligases ubiquitinating growth regulatory molecules are important because therapeutic targeting of substrate-specific E3 ligases is likely to represent a new strategy in cancer treatment (39–41).

Disclosure of Potential Conflicts of Interest

No potential conflicts of interest were disclosed.

Acknowledgments

Received 11/22/2007; revised 5/12/2008; accepted 5/21/2008.

Grant support: Swedish Cancer Society, King Gustaf V Jubilee Foundation, Swedish Medical Council, Stockholm Cancer Society, Children Cancer Society, Lundberg's Research Foundation in Gothenburg, the Stockholm County, and the Karolinska Institute.

The costs of publication of this article were defrayed in part by the payment of page charges. This article must therefore be hereby marked *advertisement* in accordance with 18 U.S.C. Section 1734 solely to indicate this fact.

References

1. Adams TE, Epa VC, Garrett TP, Ward CW. Structure and function of the type 1 insulin-like growth factor receptor. Cell Mol Life Sci 2000;57:1050–93.
2. Baserga R. Oncogenes and the strategy of growth factors. Cell 1994;79:927–30.
3. Baserga R. The insulin-like growth factor I receptor: a key to tumor growth? Cancer Res 1995;55:249–52.
4. Girnita L, Shenoy SK, Sehat B, et al. β-Arrestin is crucial for ubiquitination and down-regulation of the insulin-like growth factor-1 receptor by acting as adaptor for the MDM2 E3 ligase. J Biol Chem 2005; 280:24412–9.
5. LeRoith D, Roberts CT, Jr. The insulin-like growth factor system and cancer. Cancer letters 2003;195: 127–37.
6. Girnita L, Girnita A, Larsson O. Mdm2-dependent ubiquitination and degradation of the insulin-like growth factor 1 receptor. Proc Natl Acad Sci U S A 2003;100:8247–52.
7. Sehat B, Andersson S, Vasilcanu R, Girnita L, Larsson O. Role of ubiquitination in IGF-1 receptor signaling and degradation. PLoS ONE 2007;2:e340.
8. Vecchione A, Marchese A, Henry P, Rotin D, Morrione A. The Grb10/Nedd4 complex regulates ligand-induced ubiquitination and stability of the insulin-like growth factor I receptor. Mol Cell Biol 2003;23:3363–72.
9. Girnita L, Shenoy SK, Sehat B, et al. β-Arrestin and Mdm2 mediate IGF-1 receptor-stimulated ERK activation and cell cycle progression. J Biol Chem 2007;282:11329–38.
10. Glickman MH, Ciechanover A. The ubiquitin-proteasome proteolytic pathway: destruction for the sake of construction. Physiol Rev 2002;82:373–428.
11. Hershko A, Heller H, Elias S, Ciechanover A. Components of ubiquitin-protein ligase system. Resolution, affinity purification, and role in protein breakdown. J Biol Chem 1983;258:8206–14.
12. Vernace VA, Schmidt-Glenewinkel T, Figueiredo-Pereira ME. Aging and regulated protein degradation: who has the UPPer hand. Aging Cell 2007;6:599–606.
13. Beal R, Deveraux Q, Xia G, Rechsteiner M, Pickart C. Surface hydrophobic residues of multiubiquitin chains essential for proteolytic targeting. Proc Natl Acad Sci U S A 1996;93:861–6.
14. Hoege C, Pfander B, Moldovan GL, Pyrowolakis G, Jentsch S. RAD6-dependent DNA repair is linked to modification of PCNA by ubiquitin and SUMO. Nature 2002;419:135–41.
15. Spence J, Sadis S, Haas AL, Finley D. A ubiquitin mutant with specific defects in DNA repair and multiubiquitination. Mol Cell Biol 1995;15:1265–73.
16. Habelhah H, Takahashi S, Cho SG, Kadoya T, Watanabe T, Ronai Z. Ubiquitination and translocation of TRAF2 is required for activation of JNK but not of p38 or NF-κB. EMBO J 2004;23:322–32.
17. Haglund K, Sigismund S, Polo S, Szymkiewicz I, Di Fiore PP, Dikic I. Multiple monoubiquitination of RTKs is sufficient for their endocytosis and degradation. Nat Cell Biol 2003;5:461–6.
18. de Melker AA, van der Horst G, Borst J. c-Cbl directs EGF receptors into an endocytic pathway that involves the ubiquitin-interacting motif of Eps15. J Cell Sci 2004; 117:5001–12.
19. Diller L, Kassel J, Nelson CE, et al. p53 functions as a cell cycle control protein in osteosarcomas. Mol Cell Biol 1990;10:5772–81.
20. Masuda H, Miller C, Koeffler HP, Battifora H, Cline MJ. Rearrangement of the p53 gene in human osteogenic sarcomas. Proc Natl Acad Sci U S A 1987;84:7716–9.
21. Lee PS, Wang Y, Dominguez MG, et al. The Cbl protooncoprotein stimulates CSF-1 receptor multiubiquitination and endocytosis, and attenuates macrophage proliferation. EMBO J 1999;18:3616–28.
22. Levkowitz G, Waterman H, Zamir E, et al. c-Cbl/Sli-1 regulates endocytic sorting and ubiquitination of the epidermal growth factor receptor. Genes Dev 1998;12: 3663–74.
23. Miyake S, Lupher ML, Jr., Druker B, Band H. The tyrosine kinase regulator Cbl enhances the ubiquitination and degradation of the platelet-derived growth factor receptor α. Proc Natl Acad Sci U S A 1998;95: 7927–32.
24. Waterman H, Levkowitz G, Alroy I, Yarden Y. The RING finger of c-Cbl mediates desensitization of the epidermal growth factor receptor. J Biol Chem 1999;274: 22151–4.
25. Fuchs SY, Dolan L, Davis RJ, Ronai Z. Phosphorylation-dependent targeting of c-Jun ubiquitination by Jun N-kinase. Oncogene 1996;13:1531–5.
26. Huang F, Kirkpatrick D, Jiang X, Gygi S, Sorkin A. Differential regulation of EGF receptor internalization and degradation by multiubiquitination within the kinase domain. Mol Cell 2006;21:737–48.
27. Hu M, Li P, Song L, et al. Structure and mechanisms of the proteasome-associated deubiquitinating enzyme USP14. EMBO J 2005;24:3747–56.
28. Kee Y, Lyon N, Huibregtse JM. The Rsp5 ubiquitin ligase is coupled to and antagonized by the Ubp2 deubiquitinating enzyme. EMBO J 2005;24:2414–24.
29. McCullough J, Clague MJ, Urbe S. AMSH is an endosome-associated ubiquitin isopeptidase. J Cell Biol 2004;166:487–92.
30. Tsirigotis M, Zhang M, Chiu RK, Wouters BG, Gray DA. Sensitivity of mammalian cells expressing mutant ubiquitin to protein-damaging agents. J Biol Chem 2001; 276:46073–8.
31. Schnell JD, Hicke L. Non-traditional functions of ubiquitin and ubiquitin-binding proteins. J Biol Chem 2003;278:35857–60.
32. Sigismund S, Woelk T, Puri C, et al. Clathrin-independent endocytosis of ubiquitinated cargos. Proc Natl Acad Sci U S A 2005;102:2760–5.
33. Maggi D, Biedi C, Segat D, Barbero D, Panetta D, Cordera R. IGF-I induces caveolin 1 tyrosine phosphorylation and translocation in the lipid rafts. Biochem Biophys Res Commun 2002;295:1085–9.
34. Panetta D, Biedi C, Repetto S, Cordera R, Maggi D. IGF-I regulates caveolin 1 and IRS1 interaction in caveolae. Biochem Biophys Res Commun 2004;316: 240–3.
35. Podar K, Tai YT, Cole CE, et al. Essential role of caveolae in interleukin-6- and insulin-like growth factor I-triggered Akt-1-mediated survival of multiple myeloma cells. J Biol Chem 2003;278:5794–801.
36. Huo H, Guo X, Hong S, Jiang M, Liu X, Liao K. Lipid rafts/caveolae are essential for insulin-like growth factor-1 receptor signaling during 3T3–1 preadipocyte differentiation induction. J Biol Chem 2003; 278:11561–9.
37. Lin FT, Daaka Y, Lefkowitz RJ. β-Arrestins regulate mitogenic signaling and clathrin-mediated endocytosis of the insulin-like growth factor I receptor. J Biol Chem 1998;273:31640–3.
38. Baumann CA, Ribon V, Kanzaki M, et al. CAP defines a second signalling pathway required for insulin-stimulated glucose transport. Nature 2000;407: 202–7.
39. Weissman AM. Themes and variations on ubiquitylation. Nat Rev Mol Cell Biol 2001;2:169–78.
40. Vasilcanu R, Vasilcanu D, Rosengren L, et al. Picropodophyllin induces down-regulation of the insulin-like growth factor 1 receptor: potential mechanistic involvement of Mdm2 and β-arrestin1. Oncogene 2008; 27:1629–38.
41. Vasilcanu R, Vasilcanu D, Sehat B, et al. Insulin-like growth factor type-I receptor-dependent phosphorylation of extracellular signal-regulated kinase 1/2 but not Akt (protein kinase B) can be induced by picropodophyllin. Mol Pharmacol 2008;73:930–9.

Identification of c-Cbl as a New Ligase for Insulin-like Growth Factor-I Receptor with Distinct Roles from Mdm2 in Receptor Ubiquitination and Endocytosis

Bita Sehat, Sandra Andersson, Leonard Girnita, et al.

Cancer Res 2008;68:5669-5677.